

DETECTION OF A CIRCUMSTELLAR GAS AROUND DM TAURI: A PROTOPLANETARY DISK AROUND A SINGLE STAR?

TOSHIHIRO HANDA,¹ SHOKEN M. MIYAMA,² TAKUYA YAMASHITA,² TOSHIHIRO OMODAKA,³ YOSHIMI KITAMURA,^{4,5}
 MASAHICO HAYASHI,^{6,7} TOSHIKAZU ONISHI,⁸ RONALD L. SNELL,^{9,10} STEPHEN E. STROM,⁹ KAREN M. STROM,⁹
 MICHAEL F. SKRUTSKIE,⁹ SUZAN EDWARDS,¹¹ NAGAYOSHI OHASHI,¹² KAZUYOSHI SUNADA,¹²
 MASAO SAITO,^{6,12} YASUO FUKUI,⁸ AKIRA MIZUNO,⁸ JUN-ICHI WATANABE,²
 AND HIROKAZU KATAZA¹

Received 1994 July 18; accepted 1995 March 2

ABSTRACT

Sensitive molecular line observations carried out with the Nobeyama 45 m telescope have resulted in the detection of the ^{12}CO ($J = 1-0$) and ^{13}CO ($J = 1-0$) emission centered on the young, classical T Tauri star, DM Tau. The derived peak antenna temperatures are 0.3 K in ^{12}CO and 0.1 K in ^{13}CO . No C^{18}O emission was detected at an upper limit (3σ) of 45 mK. The emission feature has a line width of 1.7 km s^{-1} and is centered at $v_{\text{LSR}} = 5.9 \text{ km s}^{-1}$, which coincides well with the reported radial velocity for DM Tau ($5.9 \pm 2.1 \text{ km s}^{-1}$). The ^{13}CO profile shows a symmetric double peak, suggesting a Keplerian rotating disk. These observations suggest that the molecular gas is associated with and is most probably gravitationally bound to DM Tau. The derived radius of the gaseous disk is about 1000 AU using an optically thick disk model and a Keplerian rotating disk model. The gaseous mass is between 7×10^{-4} and $1 \times 10^{-3} M_{\odot}$ from the ^{13}CO intensity and the upper limit of C^{18}O intensity. Our results suggest that molecular gas is depleted from the standard gas-to-dust mass ratio or that mass distribution in the disk is steeper than the standard law, $r^{-1.5}$, although our observations cannot detect emission from an optically thick gaseous component inward of $r < 100 \text{ AU}$, if the emission comes from a Keplerian rotating disk.

Subject headings: circumstellar matter — ISM: molecules — radio lines: ISM — stars: individual (DM Tauri) — stars: pre-main-sequence

1. INTRODUCTION

Recent millimeter, submillimeter, and infrared continuum observations suggest the presence of dust disks around T Tauri stars, which have been considered to be precursors of planetary systems (Adams, Lada, & Shu 1987). At least half the low-mass pre-main-sequence stars show emission from hot micron-sized

circumstellar dust (Strom et al. 1989). Results of these observations require the dust component to be confined to a disk; otherwise the star would be invisible (Kenyon & Hartmann 1987; Bertout, Basri, & Bouvier 1988; Adams et al. 1987; Beckwith et al. 1990). Predominance of blueshifted components of the broad forbidden lines which are emitted from energetic stellar winds also suggests an inclined occulting disk around an object (Appenzeller, Jankovics, & Östreicher 1984; Edwards et al. 1987).

The size and mass are essential parameters to discuss the dynamical instability and evolution of a protoplanetary disk. In order to investigate them molecular line observation are required, because most of the dust emission comes only from the inner part ($r < 100 \text{ AU}$) of the disk and gas is usually dominated in mass. Although the 1.3 mm observations suggests that the dust masses are between 10^{-5} and $10^{-2} M_{\odot}$ (Beckwith et al. 1990), the actual total mass of the disk is quite ambiguous.

Molecular line observations enable us to refine the structure of the disk through Keplerian rotation model and spectral line synthesis (Omodaka, Kitamura, & Kawazoe 1992; Sargent & Beckwith 1991). The epoch of gas dissipation is another unresolved problem for which molecular line observations can provide the answer. Around Vega-like stars, which are main-sequence stars with IR excess due to dust emission, no molecular gas emission was found (Yamashita et al. 1993).

We have begun a survey project for gaseous disks around T Tauri stars in the Taurus-Auriga molecular clouds, which is the best region because of its vicinity (140 pc; Elias 1978) and richness of low-mass stars ($< 1 M_{\odot}$); this allows us to easily compare the results to the solar system using the Nobeyama 45 m telescope. Recently the rotating gas disk around GG Tau

¹ Institute of Astronomy, University of Tokyo, 2-21-1 Osawa, Mitaka, Tokyo 181, Japan; handa@ghz.mtk.ioa.s.u-tokyo.ac.jp, kataza@soleil.mtk.ioa.s.u-tokyo.ac.jp.

² National Astronomical Observatory, 2-21-1 Osawa, Mitaka, Tokyo 181, Japan; miyama@yso.mtk.nao.ac.jp, oyamash, owatana@c1.mtk.nao.ac.jp.

³ College of Liberal Arts, Kagoshima University, 1-21-30 Koorimoto, Kagoshima 890, Japan; omodaka@cla.kagoshima-u.ac.jp.

⁴ Department of Liberal Arts, School of Allied Medical Sciences, Kagoshima University, 8-35-1 Sakuragaoka, Kagoshima 890, Japan.

⁵ Current address: Institute of Space and Astronautical Science, 3-1-1 Yoshinodai, Sagami-hara 229, Japan; kitamura@atom1.isas.l.isas.ac.jp.

⁶ Department of Astronomy, University of Tokyo, Yayoi, Bunkyo, Tokyo 113, Japan.

⁷ Current address: National Astronomical Observatory, 2-21-1, Osawa, Mitaka, Tokyo 181, Japan; masa@optik.mtk.nao.ac.jp.

⁸ Department of Astrophysics, Nagoya University, Chikusa, Nagoya 464-01, Japan; ohnishi, fukui, mizuno@a.phys.nagoya-u.ac.jp.

⁹ Physics and Astronomy Department, University of Massachusetts, Amherst, MA 01003; snell@fcrao1.phast.umass.edu, sstrom@donald.phast.umass.edu, kstrom@hanksville.phast.umass.edu, skrutski@cannon.phast.umass.edu.

¹⁰ Five College Radio Astronomy Observatory, University of Massachusetts, Amherst, MA 01003.

¹¹ Astronomy Department, Smith College, Northampton, MA 01063; edwards@donald.phast.umass.edu.

¹² Nobeyama Radio Observatory, Minamimaki, Minamisaku, Nagano 384-13, Japan; ohashi, sunada, masao@nro.nao.ac.jp. This observation was carried out under the "long-term common use" program of the 45 m radio telescope at Nobeyama.

was found using the Nobeyama 45 m telescope (Skrutskie et al. 1993) and Nobeyama Millimeter Array (Kawabe et al. 1993). These results show that we are ready to start a quest for protoplanetary disks.

Careful criteria of source selection are required to carry out the search for protoplanetary/circumstellar gaseous disks because long integration times are required for detection. We selected the sample stars by the following two criteria.

1. CO emission from the ambient molecular cloud must be very weak, or the velocity of the star must be significantly different from that of the ambient molecular cloud. We checked the absence/weakness of ambient emission at the level of 1 K with the Nagoya 4 m telescope (160" beam), with the FCRAO 14 m telescope (45" beam), and with the Nobeyama 45 m telescope (15" beam) itself. The optical velocities are obtained by P. Hartigan & L. Ghandour (private communication).

2. The sample stars should show strong continuum emission at 1.3 mm. Strong 1.3 mm continuum sources may be rich in dust and also in molecular gas.

In this project we found CO emission associated with DM Tau. We report the first results on DM Tau in this paper. The spectral type of DM Tau is M0.5 (Strom et al. 1988). The age and mass are estimated to be $0.48 M_{\odot}$ and 1.0×10^6 yr from the H-R diagram using the tracks by D'Antona & Mazzitelli (1994) and the opacities by Alexander, Augason, & Johnson (1989) (for more about the procedure in detail, see Hartigan, Strom, & Strom 1995), or $0.62 M_{\odot}$ and 3.2×10^6 yr (Beckwith et al. 1990); in this paper, we use the former values. No companion star has been reported. The H α emission equivalent width is 140 Å (Cohen & Kuhl 1979).

2. OBSERVATIONS

The observations were made in 1992 December to 1993 March in the ^{12}CO ($J = 1-0$) line at 115 GHz using the Nobeyama 45 m telescope. The half-power beamwidth (HPBW) of the telescope is $14''.4 \pm 0''.5$ at 110 GHz, which corresponds to 2000 AU at the distance to the Taurus-Auriga dark cloud. The antenna main beam efficiency $\eta_{\text{mb}} = 0.47 \pm 0.04$ at 110 GHz. We assume the HPBW at 115 GHz is 14" and the η_{mb} is the same at 115 GHz. The position of DM Tau is $\alpha(\text{B1950.0}) = 4^{\text{h}}30^{\text{m}}54^{\text{s}}.7$, $\delta(\text{B1950.0}) = +18^{\circ}3'56''.7$ (Herbig & Bell 1988). For DM Tau we observed 21 positions in a $68'' \times 68''$ grid in equatorial coordinates (B1950.0) with a 17" spacing. A four-beam SIS receiver installed on a rotating stage was used. The typical system noise temperature was 400–550 K, including the atmospheric attenuation at zenith. The beams are separated by 34" in equatorial coordinates. Four independent 2048 channel acousto-optical spectrometers were used at the identical sky frequency. The frequency resolution is 37 kHz, corresponding to 0.096 km s^{-1} at 115 GHz.

The integrations for DM Tau were carried out in the position-switching mode. The reference position which is free of CO emission is 1° east of the stellar position in right ascension. The room temperature chopper wheel calibration (Ulich & Haas 1976) was used approximately every 20 minutes, which gives the intensity in the antenna temperature scale (T_{A}^*) after correction for atmospheric attenuation but not corrected for any beam dilution effects.

In order to calibrate the intensity scale, we observed Orion KL once each day. This calibration is required because the receiver has no single-sideband filter. We assume that the peak

antenna temperature (T_{A}^*) of Orion KL in the ^{12}CO ($J = 1-0$) line is 50 K. The correction was applied for all beams every day. The correction factor ranges between 0.96 and 2.46, but the difference depends mainly on the receiver beam; the daily change for the same beam is less than 20% during the whole observing period.

Just before and after 80 minute integration on the object, we checked the pointing calibration. This was performed by five-point mapping around an SiO maser source, NML Tau, assuming its position $\alpha = 3^{\text{h}}50^{\text{m}}43^{\text{s}}.6$, $\delta = +11^{\circ}15'32''$, using an HEMT receiver in the SiO ($J = 1-0$) line at 43 GHz. The pointing difference between the CO and SiO receivers is less than 1". For the profile at the stellar position we discarded the data for which the pointing offset differs more than 4", almost one-third of the CO beam, just before and after the integration.

A linear baseline is applied for the integrated profiles between -10 and 20 km s^{-1} with respect to the local standard of rest (LSR). The profile free of the emission is flat enough to give a well-defined linear baseline.

We also observed the ^{13}CO ($J = 1-0$) line at 110 GHz in 1993 October and 1993 December and C^{18}O ($J = 1-0$) at 109 GHz in 1993 February. The typical system noise temperature was 350–500 K in both lines. We observed six positions in ^{13}CO around the star on a 34" spacing grid and at the stellar position in C^{18}O . For the intensity calibration we assume the peak antenna temperature (T_{A}^*) of Orion KL in ^{13}CO ($J = 1-0$) is 15 K. Other specifications were the same as in ^{12}CO observations.

3. RESULTS

3.1. ^{12}CO

The profile map of ^{12}CO obtained is shown in Figure 1. The profile in each panel is separated by 17" (2400 AU) in equatorial coordinates; north is top and east is left. The central panel shows the profile at the stellar position. In all panels we find the feature at 9 km s^{-1} . We believe that this is the emission from ambient clouds, which we will discuss later. It is remarkable that the feature at 6 km s^{-1} is significant only on the stellar position. This suggests that the 6 km s^{-1} component is associated with the star. Weaker features at 6 km s^{-1} are also seen at a few positions other than the stellar position. No systematic velocity gradient was seen between these weak features and those at the stellar position.

The lower panel of Figure 2 is an enlargement of the central panel of Figure 1. After 3 hr 35 minutes integration (on+off) toward the star, this profile was obtained. The rms noise level is 38 mK in T_{A}^* . It is not clear that the feature has a double peak like GG Tau (Skrutskie et al. 1993), given the present noise level. We fit it with a single Gaussian component for the sake of simplicity. Applying this fit, the systemic velocity is found to be 5.9 km s^{-1} in LSR, and the FWHM is about 1.7 km s^{-1} . The peak antenna temperature, T_{A}^* , of the fit is 0.3 K. The integrated intensity $\int T_{\text{A}}^* dv$ is 0.5 K km s^{-1} integrated from $v_{\text{LSR}} = 4.1 \text{ km s}^{-1}$ to 7.2 km s^{-1} .

After applying a Gaussian fit, the peak velocity and the FWHM of the 9 km s^{-1} feature toward the star are 9.3 km s^{-1} and 1.1 km s^{-1} , respectively. The peak antenna temperature, T_{A}^* , is 1.1 K. The integrated intensity $\int T_{\text{A}}^* dv$ is 1.2 K km s^{-1} integrated from $v_{\text{LSR}} = 8.1 \text{ km s}^{-1}$ to 11.2 km s^{-1} .

In Figure 1 the feature at 9 km s^{-1} is seen at several positions around the star. The intensity is almost uniform in the observed region, although a large-scale intensity gradient is

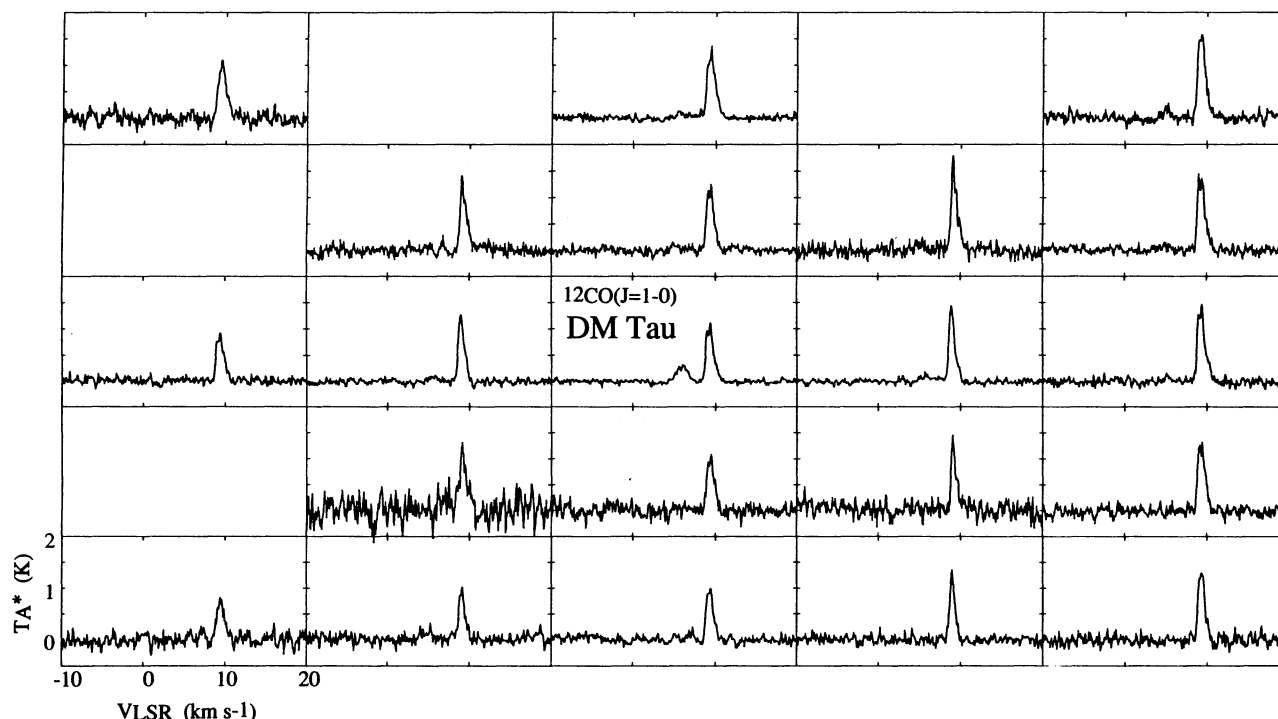


FIG. 1.— ^{12}CO ($J = 1-0$) profiles around DM Tau observed using the Nobeyama 45 m telescope. Each panel is separated by $17''$ in the equatorial coordinate (B1950.0). The central panel shows the profile toward the star. Ambient emission is seen at 9 km s^{-1} . A strong feature at 6 km s^{-1} is seen only at the star (central panel). Weaker features at 6 km s^{-1} are also seen at several other positions, which we thought to be remnant gas.

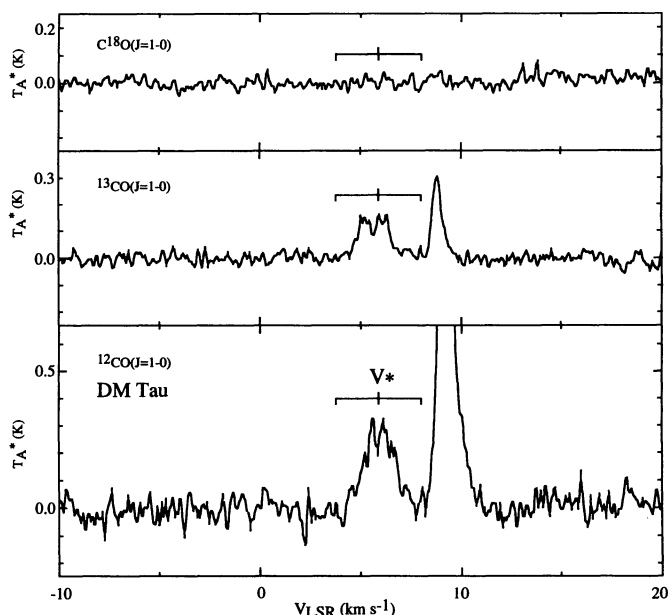


FIG. 2.—Profile at the star after 3.6 hr integration in ^{12}CO (lower panel), which is the same as the central panel of Fig. 1, after 10.5 hr integration in ^{13}CO (middle panel), and after 4.2 hr integration in C^{18}O (upper panel). The stellar velocity obtained by optical spectroscopy is indicated by v^* with an error bar. The 6 km s^{-1} feature in ^{12}CO can be well-fitted by a single Gaussian under this noise level. The 6 km s^{-1} feature in ^{13}CO shows double peaks. Velocity difference is 1.0 km s^{-1} .

seen from northwest to southeast which is consistent with the low-angular resolution map obtained with the FCRAO 14 m telescope. The 9 km s^{-1} feature is emitted by the ambient gas which has no physical interaction with the star, because the 9 km s^{-1} feature at the stellar position shows no difference from those surrounding the star. We do not discuss the 9 km s^{-1} feature again in this paper.

3.2. ^{13}CO and C^{18}O

The profiles toward DM Tau in ^{13}CO and C^{18}O are shown in the upper and middle panels of Figure 2 after 10 hr 30 minutes and 4 hr 10 minutes integration (on + off), respectively. The rms noise levels in ^{13}CO and C^{18}O are 16 mK and 15 mK in antenna temperature, respectively. Both the 6 km s^{-1} and 9 km s^{-1} features are detected in ^{13}CO , but neither are detected in C^{18}O . In ^{13}CO the 6 km s^{-1} feature shows a double peak with velocities at 5.2 and 6.2 km s^{-1} . The systemic velocity and line width are consistent with the ^{12}CO profile. The ^{13}CO profile shape is highly symmetric. The peak antenna temperature is 0.15 K for both peaks. The integrated intensity is 0.21 K km s^{-1} integrated from $v_{\text{LSR}} = 4.7 \text{ km s}^{-1}$ to 7.2 km s^{-1} .

Figure 3 shows the profile map in ^{13}CO . No ^{13}CO emission at 6 km s^{-1} can be detected except at the stellar position.

The resultant parameters of the 6 km s^{-1} feature in three isotope lines are summarized in Table 1.

4. DISCUSSION

4.1. The Feature Associated with DM Tau

The feature at 6 km s^{-1} is well confined to the position of the star. Its velocity is identical with the stellar velocity, $5.9 \pm 2.1 \text{ km s}^{-1}$ (P. Hartigan & L. Ghandour, private communication) or $4.8 \pm 1.5 \text{ km s}^{-1}$ (converted from the heliocentric velocity

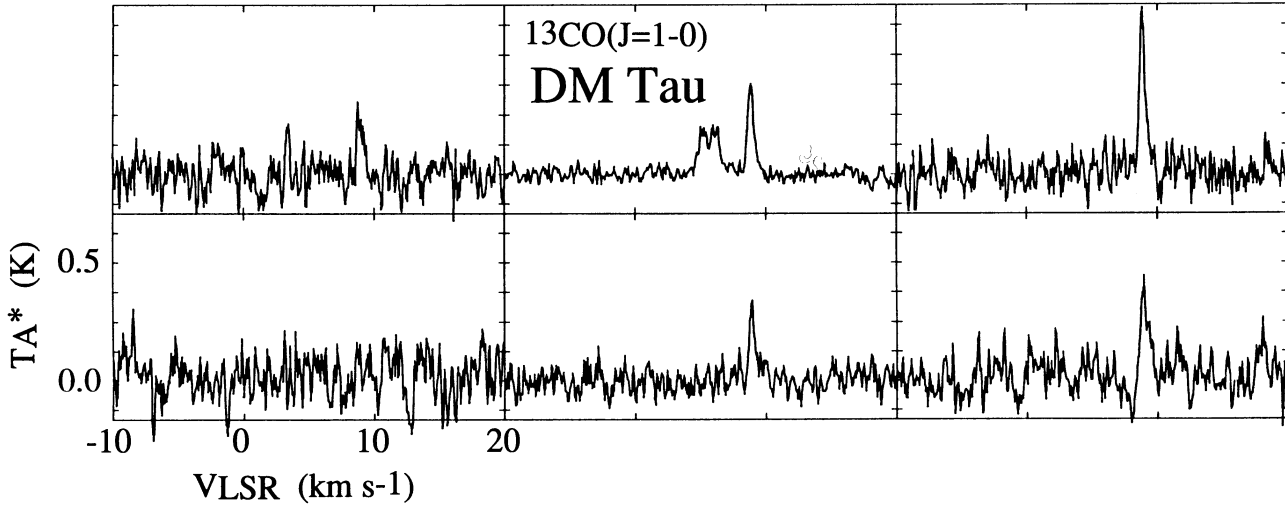


FIG. 3.— ^{13}CO profiles around DM Tau. Each panel is separated by $34''$ in the equatorial coordinate (B1950.0). The upper central panel shows the profile toward the star. No 6 km s^{-1} features are detected besides the stellar position.

by Hartmann et al. 1986), within the error. The feature at the stellar position is significantly strong, although weak features are seen at a few other positions.

We believe that the 6 km s^{-1} feature is physically associated with the star and is a circumstellar/protoplanetary disk around DM Tau for the following reasons, although the shape of the feature was not resolved with the $14''$ beam. The 6 km s^{-1} feature shows double peaks in ^{13}CO emission with 1.0 km s^{-1} velocity difference. This velocity difference is reasonable for the Keplerian rotating disk around DM Tau, but it is too small for a bipolar outflow because the velocity difference is smaller than the escape velocity of DM Tau. Moreover, high-resolution observations with the Nobeyama Millimeter Array show an elongated feature and a systematic velocity gradient along the major axis which suggests a rotating disk (Saito et al. 1995). The 1.3 mm continuum observations also suggest the existence of a dust disk around DM Tau (Beckwith et al. 1990), although the size is smaller than our gaseous disk.

At several positions besides the stellar position, marginal features at 6 km s^{-1} are also seen. No systematic trend is found for these features in the line intensity or velocity. These features may be remnants after formation of the star and its circumstellar disk. We will not discuss these features here.

4.2. Mass and Size of the Disk around DM Tau

In this section we discuss the size and mass of the disk emitting the 6 km s^{-1} feature associated with DM Tau. We will not consider depletion of CO to H_2 although Dutrey, Guilloteau, & Simon (1994) suggest the depletion of CO compared with the dust around GG Tau. Although we use the terminology for a disklike geometry in the following dis-

cussion, the estimated parameters are valid, at least within an order of magnitude, for other geometries.

We can estimate the size of the circumstellar material from the intensity of the profile. If the feature is optically thick with random velocity v_{rand} and uniform brightness of T_b , the line profile is the sum of all elements within the feature with intensity $\Delta I = T_b v_{\text{rand}} \Delta\Omega_{\text{disk}}/\Omega_{\text{beam}}$ at the velocity determined by the large-scale motion within the feature with a velocity width of v_{rand} , where $\Delta\Omega_{\text{disk}}$ and Ω_{beam} are solid angles of the element and main beam, respectively. Therefore we can estimate the size from the ^{12}CO integrated intensity through

$$\int T_A^* dv = \eta_{\text{mb}} T_b v_{\text{rand}} \Omega_{\text{disk}}/\Omega_{\text{beam}}, \quad (1)$$

where Ω_{disk} is the solid angle of the feature. If the geometry of the feature is a flat disk, then $\Omega_{\text{disk}} = \pi r_{\text{disk}}^2 \cos i$, where r_{disk} is a disk angular radius and i is the inclination of the disk ($i = 0$ for face-on). For the Gaussian beam $\Omega_{\text{beam}} = 1.133\theta_{\text{HPBW}}^2$. Although the thermal line width of CO at 20 K is 0.2 km s^{-1} , the typical line width of a dark cloud is broader than it and is about $1\text{--}5\text{ km s}^{-1}$. The v_{rand} must be narrower than the FWHM of the 6 km s^{-1} feature, 1.7 km s^{-1} , if systematic rotation dominates. We assume $v_{\text{rand}} = 0.5\text{ km s}^{-1}$ and $T_b = 20\text{ K}$. The derived radius using equation (1) is 540 AU ($i = 60^\circ$) or 380 AU ($i = 0$; face-on). The solid angle of the feature is the same as Ω_{disk} even if the feature is not disklike.

Another estimate of the disk size is derived from the velocity width of the profile based upon a rotating Keplerian disk using

$$r_{\text{disk}} = \frac{4GM_* \sin^2 i}{v_{\text{FW}}^2} \quad (2)$$

where G is the gravitational constant, M_* is the stellar mass, v_{FW} is the full velocity width of the outermost part of the disk with a radius r_{disk} . The value of M_* for DM Tau is $0.48 M_\odot$. Assuming the v_{FW} is equal to the velocity difference between the two peaks in ^{13}CO emission, 1.0 km s^{-1} , the typical disk radius is 1300 AU ($i = 60^\circ$) or 1700 AU ($i = 90^\circ$; edge-on).

In order to evaluate the radius of the inner part of the disk from which we do not measure the emission, we can use the full width of the profile. The full width at the first null is about 3.5 km s^{-1} . If we assume a Keplerian rotating disk about a 0.48

TABLE 1

6 km s^{-1} FEATURE FROM DM TAURI

Transition	Peak T_A^* (K)	Peak Velocity (km s^{-1})	Integrated Intensity (K km s^{-1})	rms Noise (mK)
$^{12}\text{CO} (J = 1-0)$	0.3	5.9	0.5	38
$^{13}\text{CO} (J = 1-0)$	0.15	5.2, 6.2	0.21	16
$\text{C}^{18}\text{O} (J = 1-0)$	<0.045	15

M_{\odot} star with an inclination of 60° , then the detected profile is emitted from the gaseous component of the disk beyond 100 AU, which is beyond the radius of the orbit of Pluto, 40 AU. Therefore our estimate of the gaseous mass of the disk applies only to the outer part ($r > 100$ AU) of this structure.

The lower limit to the molecular mass of the disk is estimated from the integrated intensity of ^{13}CO based upon the assumption of optically thin emission. From the ^{13}CO ($J = 1-0$) line we can estimate the column density of ^{13}CO molecules in cm^{-2} through

$$N(^{13}\text{CO}) = 2.42 \times 10^{14} \frac{\int T_A^*(^{13}\text{CO})/\eta_{\text{mb}} dv}{1 - \exp(-5.29/T_{\text{ex}})}, \quad (3)$$

where $\int T_A^*(^{13}\text{CO})/\eta_{\text{mb}} dv$ is the integrated mainbeam brightness temperature of the ^{13}CO ($J = 1-0$) line in K km s^{-1} and T_{ex} is the gas excitation temperature in K. It is difficult to evaluate the gas excitation temperature directly from observations. Using CO data observed by Skrutskie et al. (1993), Kitamura et al. (1993) estimated the gas temperature of the gaseous circumstellar disk around GG Tau to be 13 K at 500 AU and 30 K at 100 AU. Using 1.3 mm continuum data observed by Beckwith et al. (1990) and their equation (8), the dust temperature around DM Tau is estimated to be 108 K at 1 AU and 10 K at 100 AU. We assume T_{ex} to be 20 K in this paper. The number ratio of $N(\text{H}_2)/N(^{13}\text{CO})$ is assumed to be 9×10^5 (Schloerb & Snell 1984). The derived lower mass limit of the 6 km s^{-1} feature in the $14''.4$ beam is $7 \times 10^{-4} M_{\odot}$.

Using the upper limit of the C^{18}O emission, we can estimate an upper mass limit for the 6 km s^{-1} feature. Using an upper limit of intensity, 3σ of, 45 mK, and the expected FWHM the same as that of ^{12}CO emission, 1.7 km s^{-1} , the upper limit of the integrated intensity of C^{18}O is 0.08 K km s^{-1} assuming the Gaussian line shape. From the C^{18}O ($J = 1-0$) line, we can estimate the column density of C^{18}O molecules through

$$N(\text{C}^{18}\text{O}) = 2.43 \times 10^{14} \frac{\int T_A^*(\text{C}^{18}\text{O})/\eta_{\text{mb}} dv}{1 - \exp(-5.27/T_{\text{ex}})}, \quad (4)$$

where $\int T_A^*(\text{C}^{18}\text{O})/\eta_{\text{mb}} dv$ is integrated mainbeam brightness temperature in the C^{18}O ($J = 1-0$) line in K km s^{-1} and T_{ex} is the gas excitation temperature in K. The number ratio of $N(\text{H}_2)/N(\text{C}^{18}\text{O})$ used is 4×10^6 (Duvert, Cernicharo, & Baudry 1986). Assuming the gas excitation temperature T_{ex} to be 20 K, the derived upper mass limit of the 6 km s^{-1} feature in our $14''.4$ beam is $1 \times 10^{-3} M_{\odot}$. Therefore, the gaseous mass is between $7 \times 10^{-4} M_{\odot}$ and $1 \times 10^{-3} M_{\odot}$ if the abundance of the CO gas is not depleted. Note that these estimations are valid only for the outer part of the disk ($r > 100$ AU) in the previous discussion.

Using the millimeter-wave continuum, the mass of the disk around DM Tau can be derived. The dust continuum from the disk is 109 mJy at $\lambda = 1.3 \text{ mm}$. The estimated total mass of the disk is $0.034 M_{\odot}$ assuming the typical interstellar dust-to-gas mass ratio (Beckwith et al. 1990). This is nominally more massive than our derived disk mass by a factor of 30. However, the discrepancy does not directly imply gas depletion from the disk because the masses derived from these two methods are based upon emission from different annuli of the disk. Because of antenna dilution and dilution in the velocity domain due to rapid rotation in the inner regions of the disk, we cannot estimate the gaseous mass in the inner part ($r < 100$ AU) of the disk. The continuum observations demonstrate that an optically thick disk at millimeter wavelengths exists around DM

Tau inside $r = 13$ AU and that the mass derived from these observations is dominated by the inner part ($r < 20$ AU) of the disk (Beckwith et al. 1990). However, the mass in the outer region ($100 \text{ AU} < r < 1000 \text{ AU}$) is more massive than that in the inner region ($r < 100 \text{ AU}$) if the mass distributes as $r^{-1.5}$ (Hayashi 1981; Beckwith et al. 1990) by a factor of 2. Therefore, a discrepancy of a factor of 30 suggests either that the molecular gas (at least CO gas) is depleted compared with the dust from typical interstellar gas or that mass distribution on the disk is steeper than the standard law, $r^{-1.5}$.

More accurate parameters will be derived by fitting the data with more realistic models in a forthcoming paper (Kitamura et al. 1995).

4.3. Comparison to the Disk around GG Tau

The first T Tauri star associated with molecular line emission from a circumstellar disk was GG Tau (Kawabe et al. 1993; Skrutskie et al. 1993). From the results of the ^{12}CO and C^{18}O observations from the Nobeyama 45 m telescope by Skrutskie et al. (1993), the radius of the disk around GG Tau using equation (1) is 770 AU if the inclination of 60° or 540 AU if the disk is face-on. Using equation (2) and the recalculated stellar mass of $0.28 M_{\odot}$ (see the next paragraph), we find a radius as 610 AU with $i = 60^{\circ}$ or 820 AU if the disk is viewed edge-on. Using equation (4) and the corresponding equation for ^{12}CO with the same physical parameters as used in this paper, the upper mass limit in the $14''$ beam is recalculated to be $1.1 \times 10^{-3} M_{\odot}$ and the lower mass limit is calculated to be $7.1 \times 10^{-6} M_{\odot}$. Based upon the results by Skrutskie et al. (1993), Kitamura et al. (1993) estimated more precise parameters for the disk around GG Tau. Their estimated gaseous mass is less than $0.003 M_{\odot}$ and the disk radius is 900 AU at an inclination of 67° . Comparing their results with our estimations leads us to believe that our rough estimations are correct to within an order of magnitude.

Our results suggest that the size and mass of the gaseous disk around DM Tau are similar to those of the disk around GG Tau. The stellar mass and age of GG Tau, using the tracks by D'Antona & Mazzitelli (1994) and the opacities by Alexander et al. (1989), are $0.28 M_{\odot}$ and $4.3 \times 10^4 \text{ yr}$, respectively (for the procedure in detail, see Hartigan et al. 1995), which are considerably less massive than the values used by Beckwith et al. (1990), $0.65 M_{\odot}$ and $3 \times 10^5 \text{ yr}$. The stellar mass of DM Tau is only 1.5 times that of GG Tau, but DM Tau appears to be 25 times older than GG Tau. However, the disk around DM Tau does not appear to have evolved significantly over this great time span. According to the Kyoto model, the gas in a protoplanetary disk is dissipated at approximately 10^7 – 10^8 yr after the birth of the central star (Hayashi, Nakazawa, & Nakagawa 1985). The Kepler times of DM Tau and GG Tau are larger than that of the Sun only by a factor of 1.6 and 1.9, respectively. Both the disks around DM Tau and GG Tau may be before the gas dissipation stage.

A close companion star is reported for GG Tau using IR-speckle observations (Leinert et al. 1991), but no companion has been seen for DM Tau. However, we find no significant difference between the gas disks around DM Tau and GG Tau. Recently Dutrey et al. (1994) reported a hole of the dust disk around GG Tau by direct imaging. They suggest that this hole may be formed by the companion star through dynamical effects. High-resolution imaging of DM Tau is very important in order to evaluate the effects of binarity.

5. CONCLUSIONS

During the survey for circumstellar disks around T Tauri stars in the Taurus-Auriga region, we have found molecular line emission toward DM Tau. The results show that the gaseous disk around the star is 1000 AU in radius and 10^{-3} to $10^{-4} M_{\odot}$ for the outer disk ($r > 100$ AU). The size and mass of the disk around DM Tau are comparable to those of the disk around GG Tau, although DM Tau appears to be 25 times older than GG Tau and has no companion star. Our results suggest that molecular gas is depleted from the standard

gas-to-dust mass ratio or that mass distribution in the disk is steeper than the standard law, $r^{-1.5}$, although our observations cannot detect emission from an optically thick gaseous component inward of $r < 100$ AU, if the emission comes from a Keplerian rotating disk.

We wish to thank P. Hartigan and L. Ghandour for providing the optical velocity of DM Tau. We also thank the staff in the Nobeyama Radio Observatory for the operating of the 45 m telescope.

REFERENCES

- Adams, F. C., Lada, C. J., & Shu, F. H. 1987, *ApJ*, 312, 788
 Alexander, D. R., Augason, G. C., & Johnson, H. R. 1989, *ApJ*, 345, 1014
 Appenzeller, I., Jankovics, I., & Östreicher, R. 1984, *A&A*, 141, 108
 Beckwith, S. V. W., Sargent, A. I., Chini, R. S., & Güsten, R. 1990, *AJ*, 99, 924
 Bertout, C., Basri, G., & Bouvier, J. 1988, *ApJ*, 330, 350
 Cohen, M., & Kuhl, L. V. 1979, *ApJS*, 41, 743
 D'Antona, F., & Mazzitelli, I. 1994, *ApJS*, 90, 467
 Dutrey, A., Guilloteau, S., & Simon, M. 1994, *A&A*, 286, 149
 Duvert, G., Cernicharo, J., & Baudry, A. 1986, *A&A*, 164, 349
 Edwards, S., Cabrit, S., Strom, S. E., Heyer, I., Strom, K. M., & Anderson, E. 1987, *ApJ*, 321, 473
 Elias, J. H. 1978, *ApJ*, 224, 857
 Hartigan, P., Strom, K. M., & Strom, S. E. 1995, *AJ*, in press
 Hartmann, L., Hewett, R., Stahler, S., & Mathieu, R. D. 1986, *ApJ*, 309, 275
 Hayashi, C. 1981, *Prog. Theor. Phys. Suppl.*, 70, 35
 Hayashi, C., Nakazawa, K., & Nakagawa, Y. 1985, in *Protostars & Planets II*, ed. D. C. Black & M. S. Matthews (Tucson: Univ. of Arizona Press), 1100
 Herbig, G. H., & Bell, K. 1988, *Lick Obs. Bull.*, No. 1111
 Kawabe, R., Ishiguro, M., Omodaka, T., Kitamura, Y., & Miyama, S. M. 1993, *ApJ*, 404, L63
 Kenyon, S. J., & Hartmann, L. 1987, *ApJ*, 323, 714
 Kitamura, Y., et al. 1995, in preparation
 Kitamura, Y., Omodaka, T., Kawabe, R., Yamashita, T., & Handa, T. 1993, *PASJ*, 45, L27
 Leinert, Ch., Haas, M., Richichi, A., Zinnecker, H., & Mundt, R. 1991, *A&A*, 250, 407
 Omodaka, T., Kitamura, Y., & Kawazoe, E. 1992, *ApJ*, 396, L87
 Saito, M., Kawabe, R., Ishiguro, M., Miyama, S. M., Hayashi, M., Handa, T., Kitamura, Y., & Omodaka, T. 1995, *ApJ*, in press
 Sargent, A. I., & Beckwith, S. V. W. 1991, *ApJ*, 382, L31
 Schloerb, F. P., & Snell, R. L. 1984, *ApJ*, 283, 129
 Skrutskie, M. F., et al. 1993, *ApJ*, 409, 422
 Strom, K. M., Strom, S. E., Edwards, S., Cabrit, S., & Skrutskie, M. F. 1989, *AJ*, 97, 1451
 Strom, K. M., Strom, S. E., Kenyon, S. J., & Hartmann, L. 1988, *AJ*, 95, 534
 Ulich, B. L., & Haas, R. W. 1976, *ApJS*, 30, 247
 Yamashita, T., Handa, T., Omodaka, T., Kitamura, Y., Kawazoe, E., Hayashi, S. S., & Kaifu, N. 1993, *ApJ*, 402, L65